



# Simply Structured Wearable Triboelectric Nanogenerator Based on a Hybrid Composition of Carbon Nanotubes and Polymer Layer

Meng Su<sup>1</sup> · Juergen Brugger<sup>2</sup> · Beomjoon Kim<sup>1</sup>

Received: 16 September 2019 / Revised: 8 March 2020 / Accepted: 10 March 2020 / Published online: 3 April 2020  
© Korean Society for Precision Engineering 2020

## Abstract

Triboelectric nanogenerators (TENGs) have proven to be a robust power source for efficiently converting environmental mechanical energy into electricity. Triboelectric technology experienced substantial growth in the past few years, especially in the field of green wearable power sources as the Internet of Things develops. However, it is still difficult to overcome some remaining bottlenecks for wearable TENGs, such as limited choice of materials, unsafe metal electrodes, complex structures, and finally an insufficient electrical output. In this work, we present a simply structured wearable TENG that delivers usable electric power based on human motion. The form of TENG, which combines a friction material of silk and an electrode material of carbon nanotube (CNT) in liquid phase to achieve a biodegradable conductive mixing friction layer is new and unique. A series of delicate investigative experiments were conducted to clarify the impacts of various parameters and their optimal values in the fabrication. Then the special mixing layer was attached to a glove and tested with various daily actions, showing high potential as a power source for wearable electronics and as a motion sensor itself. This new form of CNT-silk TENG will push the field's development toward actual use, with lower cost and less burden for both of production and usage, with the advanced features of high softness, high sensibility, light weight, and simple structure.

**Keywords** Triboelectric nanogenerator · Wearable power supply · Silk fibroin · Carbon nanotube composite · Simple structure

## 1 Introduction

Electronic devices and systems have experienced exponential growth during the past decades while gradually becoming a part of people's daily life. With the development of "top-down" manufacturing technologies, the dimensions and power consumption of autonomous electronic devices and systems have decreased significantly. In the same time, electronic devices become more diverse, offering more comprehensive and vital functions, and requiring for increased

power consumption [1, 2]. In particular, wearable sensors and electronics, which provide convenience and security to society, are facing the issue of power supply [3, 4]. Batteries are always the first choice. However, they cause severe environmental problems, and lack the required properties of flexibility, comfort, lightweight, convenience and uniform specification for wearability. Energy harvesting technologies that convert ambient power into electricity are promising solutions for relieving the burdens of environmental safety and physical comfort. As different mechanisms of piezoelectricity, thermoelectricity, photoelectricity and the electromagnetic effect focused on wearables rapidly developing [5–9], an emerging mechanism of triboelectricity has attracted a lot of attention in recent years.

The triboelectric nanogenerator (TENG) equips outstanding properties of high efficiency, environmental friendliness, economic universality and widespread availability [10, 11]. By combining contact charging and electrostatic induction, TENG is able to convert irregular and low-frequency human motion into electrical charges, and then to generate current when connected with external circuits [12]. The output of

---

**Electronic supplementary material** The online version of this article (<https://doi.org/10.1007/s40684-020-00212-8>) contains supplementary material, which is available to authorized users.

---

✉ Meng Su  
sumeng@iis.u-tokyo.ac.jp

<sup>1</sup> CIRMM, Institute of Industrial Science, The University of Tokyo, Tokyo 153-8505, Japan

<sup>2</sup> Microsystems Laboratory, École Polytechnique Fédérale de Lausanne, 1015 Lausanne, Switzerland

TENG device has fundamentally high electric potential even with low current ( $\mu\text{A}$  level). Such characteristics make it have a strong sensitivity, and even a very slight movement can produce a visible electrical output, and the weak current will not pose a threat to the human body [13]. In the wearable field, although many micro-sensors consume little power, they need to be used very frequently and may even be used in real time to monitor human conditions [14, 15]. With the high applicability and security, by employing several working modes and structures, TENGs have acted as many kinds of motion sensors on different parts of the body, thanks to their soft friction materials, and the fact that pulse signals are readily discernible [16–18]. TENGs are now gradually becoming the first choice among contenders as a wearable power supplying source [19, 20], because a power source that can release a small amount of available electrical energy frequently would be more practical than a power source that has large energy storage but a burden on the human body and a difficulty of charging quickly. TENGs' advantages of being easy to integrate, economical to fabricate and process, able to efficiently and safely deliver usable output are bringing more and more broad application prospects in various forms [21–23].

Although there already exist many remarkable results for the field of wearable TENGs [24–27], certain bottlenecks are still difficult to overcome. First, synthetic materials such as nylon [28], polyester [29, 30], silicon rubber [31–33], and polydimethylsiloxane (PDMS) [34, 35] are generally used. Most of them are not soft nor breathable enough, leading to a low wear comfort. Second, metals such as copper, silver, gold and nickel have always been the researcher's choices for TENG electrodes, but such metals impose the risk of allergy, and are not suitable for clothing that is in direct contact with human skin [36]. More importantly, conventional TENGs usually needed a long and complicated fabrication procedure to achieve wearability, because their metal electrodes and synthetic, inflexible friction materials were originally hard to wear [37]. This processing induces high cost and difficulties for widespread application, and restricted further development of TENG use in daily life. Last, the output of the TENGs needs to be high enough to meet wearable electronics' specifications as a qualified power source.

In this work, a simply structured wearable TENG that delivers usable electric power based on human body motion is proposed, utilizing natural skin-friendly silk as the friction material and non-metallic carbon nanotubes (CNTs) as the electrode material. This form of a TENG, which combines a friction material (silk) and electrode material (CNT) in the liquid phase to achieve a biodegradable CNT-silk composite is very unique. Compared to the other existed composite-based TENG [38, 39], equipping both usable electrical conductivity and good power generation performance is another crucial innovative point of the proposed device. Herein, we

show in-depth and systematic experiments to elucidate the influence of various processing techniques, as well as the parameters on the power generation performance. Our proposed CNT-silk composite is capable to reach high output power as shown by using a dedicated vibration platform for quantitative power generation assessment, as well as random human body motion (i.e. finger typing). The later will support the exploration of lower cost and less burden for both of production and use, with the advanced features of high softness, light weight, and simple structure.

## 2 Methods

### 2.1 Preparation of CNT-Silk TENG

#### 2.1.1 Material Selection of Silk and CNT

This paper aims to make a TENG from materials that are truly wearable and that can be easily afforded. Silk is very light in weight, comfortable to wear, moisture absorbing and breathable, and is widely used for weaving into various satin and knitwear. Moreover, silk is easy to be positively charged during friction, being proved already to be suitable for triboelectric power generation [40]. Because silk fibroin is a natural animal protein, it is very easy to process and mix with other substances. Other materials that have better power generation performance (“+” positive side) are inferior in terms of softness and workability. Therefore, silk is a promising material for a low cost and highly available wearable TENG device.

As for electrode material, metals have danger to cause metal allergy, and need much efforts to be processed into thin and fine fibers, leading to high cost and complicated procedures. Multi-walled carbon nanotube is one of the most inexpensive choice for non-metallic conductive material. The component is simple and pure, and the commercialized powder provides much convenience in the following metering and mixing experiments.

The combination of the two materials is highly controllable, and the single layer structure equips high adaptability. As shown in Fig. 1a, the CNT-silk layer is connected to the ground through electronics, showing that it does not need to form a loop with other friction side, greatly reducing the burden of wear. Any object from the outside can freely form a friction pair with it.

The CNT-silk membrane has a unique microstructure. The silk is wrapped with carbon nanotubes like a layer of shell, as shown in Fig. 1b, c, making the surface of the overall film smooth, dense and tight. The carbon nanotubes act as electrode, connect with each other, and form a microscopic porous structure for the mixing film, which increases the

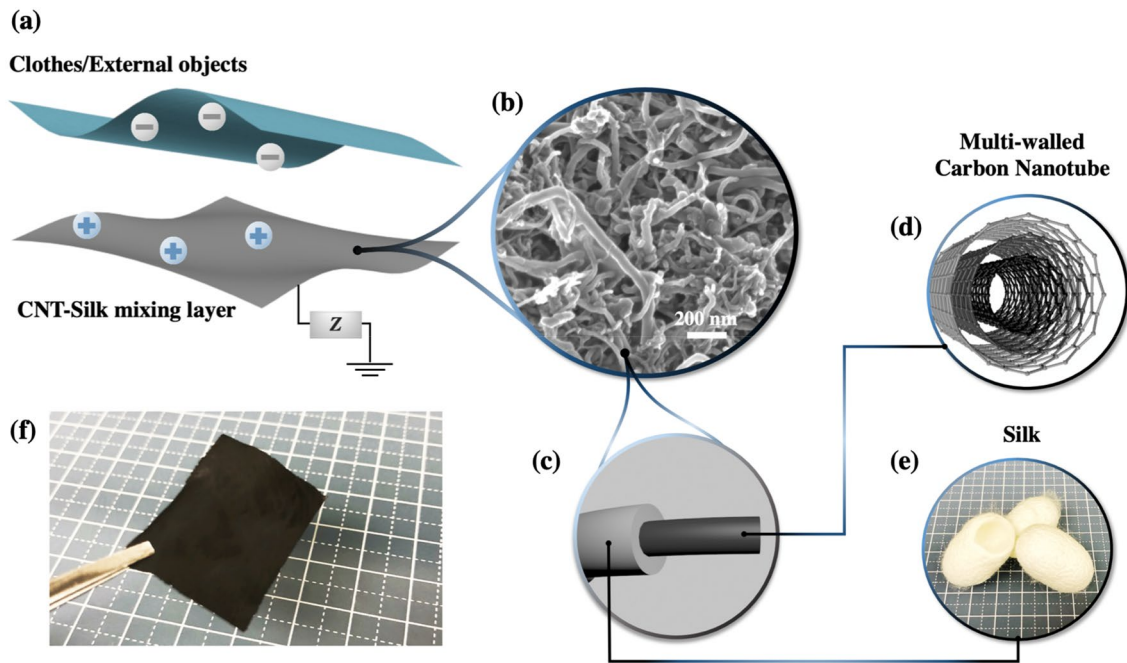


**Fig. 1** **a** The schematic view of the CNT-silk mixing layer based TENG. The CNT-silk mixing layer is easily to be positively charged during frictions with other cloth materials and external objects such as air. The potential drops between the two friction layers will drive electrons to flow from the CNT-silk layer to the ground, powering up electronics connected in between. **b** The SEM view of the surface

of the CNT-silk layer. **c** The combining structure of CNT and silk fibroin. The inner core of the tube-shaped structure is consisted by **d** multi-walled carbon nanotubes, which is the electrode of the TENG; and the outer cover is formed by **e** silk, which acts as the triboelectric material. **f** The optical image of a piece of the proposed CNT-silk mixing membrane

friction efficiency. The whole piece of solid film is shown in Fig. 1f.

### 2.1.2 Preparation of CNT-Silk Mixing Solution

100 mg of multi-walled CNT powder (Sigma-Aldrich, > 98% carbon basis, 6–13 nm × 2.5–20 μm) was added to 20 g of formic acid (Sigma-Aldrich, 88–91%), and the mixture was then shaken for 3 h in an ultrasonic bath to obtain a CNT-formic acid mixing solution of 4 mg/ml. On the other hand, an aqueous solution of silk fibroin was prepared using the method presented by Refs. [41–43], and is briefly summarized as follows. *Bombyx mori* cocoons that are bound together by sericin were boiled in 0.02 M sodium carbonate (Na<sub>2</sub>CO<sub>3</sub>) solution for 45 min to be degummed. The obtained silk fibres were then rinsed by distilled (DI) water and put to air dry at room temperature for 24 h. Then the silk fibres were dissolved in 9.3 M lithium bromide (LiBr) solution at 60 °C and kept at this temperature for 3 h to be completely dissolved. Next, the LiBr was removed by dialysis (3.5 K MWCO, Slide-A-Lyzer Dialysis Cassette, Thermo Fisher Scientific Inc.) for 72 h. Next, the silk fibroin solution was purified by twice of 20 min centrifugation step, then followed by microfiltration (5 μm, Millipore Inc.). In our case, 4.2 wt% (40 mg/ml) silk fibroin solution was obtained when

using a 13 wt% silk-LiBr solution. In order to avoid the protein denaturation, the silk fibroin solution was stored at 4 °C and was used within 1 week after preparation. Finally, the silk fibroin solution was added to the CNT-formic acid solution, and then shaken for 2 h in an ultrasonic bath to obtain the silk fibroin-CNT-formic acid mixing solution.

### 2.1.3 Fabrication of PET-Substrate CNT-Silk TENG

In this study, in order to verify the effectiveness of this new structure of a mixing layer, polyethylene terephthalate (PET), which is a very common and inexpensive material with excellent performance in triboelectric energy harvesting, was used to simulate the external friction materials (i.e. clothing) during friction.

Here, the design of the PET-substrate testing TENG device follows an arch-shaped geometry, as shown in Fig. 2a, which has been proven to function as an efficient mechanical structure for a reliable-performance TENG [44]. This vertical-contact mode is simple in structure, convenient to manufacture and repair, less harmful to the friction surface, and can be well used on a vibrating shaker to test power generation performance. In this case, two 200 μm PET/Indium tin oxide (ITO) foils (Thorlabs, OCF2520) were utilized as the supporting structures, with the PET films bent into an

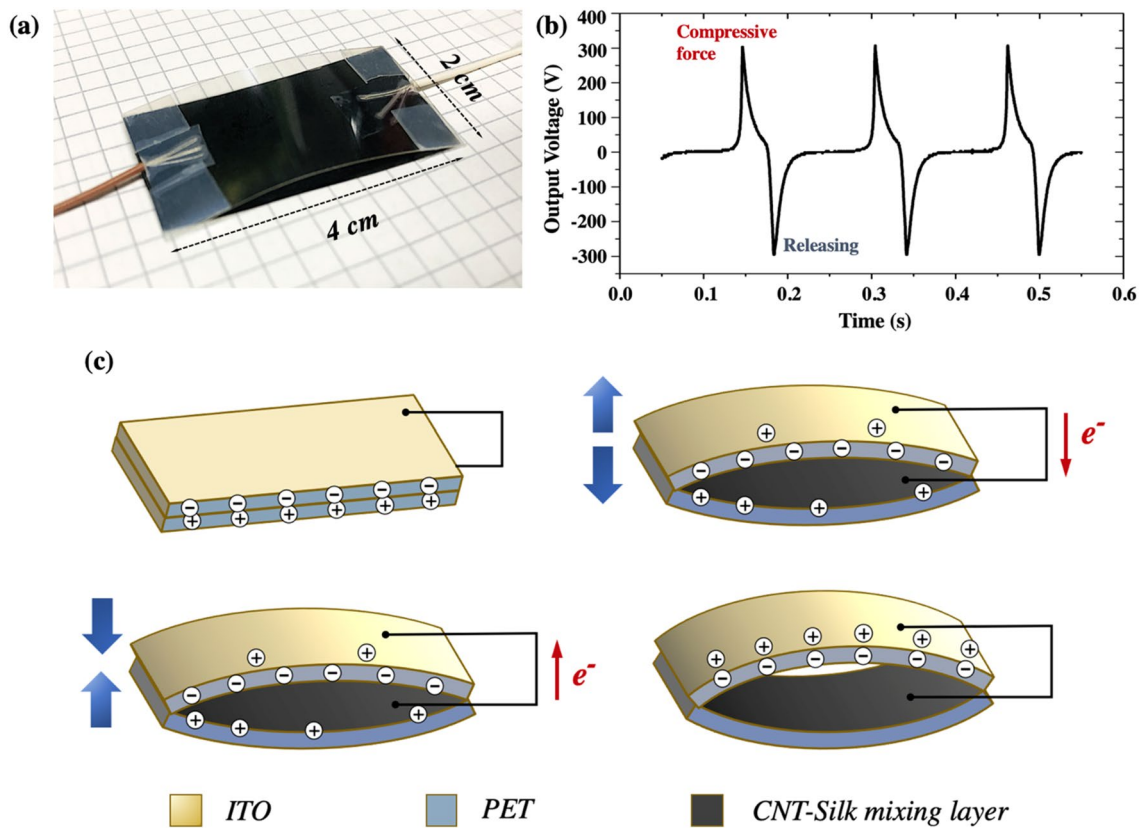


**Fig. 2** **a** The optical image of the PET-substrate testing TENG. This device was used to simulate the friction condition with CNT-silk membrane, in order to test its power generation capability. **b** The circles of power generation waveform under the repeated patting of vibrational shaker. **c** The schematic view of the shape and working

mode of the PET-substrate testing TENG. One side of the friction pair is the CNT-silk layer, which acts as friction material and electrode simultaneously. The other side is the PET/ITO film, wherein PET acts as friction material, and ITO acts as electrode

arch shape and affixed by elastic tapes, with the  $300 \Omega/\square$  ITO layers serving as PET's electrodes. One of the PET surfaces was treated with 5 min of oxygen plasma with 30 W of RF power (YHS-R/Sakigake Semiconductor Co., Ltd.). Subsequently, the CNT-silk mixing solution was coated tightly onto the PET surface, and the mixing layer itself served as its electrode. In this way, the CNT-silk mixing layer and the other side of the PET constituted the triboelectric pair of the designed testing TENG.

## 2.2 Tests and Measurements

A vibration platform was set up for systematic study of the electrical properties and energy harvesting efficiency of the fabricated CNT-silk testing TENG. Firstly, a functional generator (SG-4105, IWATSU Electric Co., Ltd) was used to generate a 7 Hz electrical signal with an amplitude of 1.3 V, which was subsequently enlarged by an amplifier (MA1, IMV Corp.) Then the amplified signal was utilized to drive a vibrational shaker (m060, IMV Corp.), and then

a 7 Hz periodic vibration with the amplitude of 35 mm was obtained. An aluminium mass was tightly fixed onto the shaker to provide the vibrational external force to the testing TENG placed underneath the mass. More details are shown in the supporting information section. The optical properties of the fabricated CNT-silk/PET/ITO layers were studied using a UV-Vis-NIR spectrophotometer (V-670, JASCO International Co., Ltd.). The surface morphology was tested by a Laser Scanning Microscope (VK-8700 Keyence Corp.) The sheet resistance was tested using a 4-point sheet resistance tester ( $0.01 \text{ m}\Omega/\square$ – $5000 \text{ k}\Omega/\square$ . K-705RS Kyowariken Corp.). Additionally, a digital oscilloscope (TDS2024, Tektronix Inc.) with a probe of  $100 \text{ M}\Omega$  (100:1 probe, Hioki 9666) was used to measure the generated output voltage and current of the TENGs. All experimental data were collected after the output of TENG stabilized to avoid deviations due to separation distance and initial charge on the device. All our experiments were carried out in ambient air, at room temperature of  $22^\circ \text{C}$  under the relative humidity of  $\sim 30\%$ .

## 3 Results and Discussion

### 3.1 Power Generation Mechanism

The output cycle is shown in Fig. 2b, when the device was directly connected to oscilloscope with a matched load of 30 M $\Omega$ . With random contact between CNT-silk film and PET, charges are generated and trapped on the PET surfaces. When the PET is pulled away from the mixing film, the electrical field balance due to the surface charges is destroyed, causing a change in the potential difference. This potential difference drives electrons to flow through external circuits to form an electric current. When the PET approaches the mixing membrane again, the potential difference will drive the electrons to flow in the opposite direction to achieve equilibrium.

In the case of the PET-substrate testing TENG, the potential drop generated during friction will drive electrons to flow between CNT-silk film and ITO electrode layer, as shown in Fig. 2c. This mode is less affected by external noise and was therefore used to test the power generation performance of the mixing layer. And the case of the proposed single-electrode mode was adopted in the later application section. In that case, the CNT-silk film is connected directly to the ground, allowing the same potential drop to drive electrons to flow in between. With this mechanism, the CNT-silk film together with PET forms a power source, turning the mechanical energy into electricity.

### 3.2 Effect of Different Weight Ratios Between Silk and CNT

The CNT-silk solution consisted of the two components of silk fibroin and CNT with formic acid solvent and little DI water. Different weight ratios of the two components of silk and CNT were used in each solution sample, as follows:

$$M_{\text{CNT}} : M_{\text{Silk fibroin}} = 5 : 1, 3 : 1, 1 : 1, 1 : 3, 1 : 5$$

Because the microstructure of CNT and silk fibroin are completely different, and they neither react nor agglomerate with each other, the two components tended to separate from each other and group together with particles of the same kind as the solvent evaporated. This phenomenon of agglomeration has always occurred during difficult CNT's dispersion in previous researches [45], as shown in Fig. 3c. Agglomeration phenomenon has a negative impact on the conductivities and final performance of the CNT-silk layer. This effect can be intuitively reflected in the testing with CNT-silk droplets. As shown in the Fig. 3a, drops of the solutions with different weight ratios showed different morphology after drying naturally. Of these dried residues, only

the samples with ratios 5:1, 3:1, and 1:1 were conductive. The other samples 1:3 and 1:5 contained more silk fibroin, leading to severe agglomeration of CNTs and poor conductivity, and were not able to achieve any conductivity to serve as an electrode and triboelectric layer simultaneously.

The same volume of each conductive solution was then evenly drop-coated by syringe on a PET substrate of 8 cm<sup>2</sup>, as described in the former section, to fabricate the testing TENGs, as shown in Fig. 3b. As the ratio changed, the degree of agglomeration also varied. In this study, evaluations were performed by measuring the surface roughness, surface sheet resistance and power generation effect of different samples. Surface roughness and sheet resistance were used to evaluate the severity of the agglomeration phenomenon—the more even the surface, the less severe the agglomeration, and the better conductive performance would be achieved. Together with the results shown in Fig. 3d, e, when the ratio was 1:1, the CNT-silk film has the best mixed dispersion state and sufficient conductivity to achieve the requirements. The sheet resistance of the mixing film has the same order of magnitude ( $\Omega/\square$ ) as the sheet resistance of ITO, so its conductivity is within an acceptable range. And the results shown in Fig. 3f indicated that the weight ratio of  $M_{\text{CNT}}:M_{\text{Silk}}$  of 1:1 performed best in generating electric power under the same conditions, which preferentially affected the choice of the optimal ratio. Combining all the test results, 1:1 was set as the optimal and default ratio during the following tests.

### 3.3 Effect of Different Coating Methods of the Mixing CNT-Silk Solution

In this research, different coating methods will cause different durability and electric performance of the CNT-silk films. Here, several different coating methods were employed to coat the same amount of mixing solutions on PET substrates of the same size. The first method was using a syringe to conduct drop coating, according to the schematic shown in Fig. 4a. The second way was using a wire bar coater to conduct slide coating, as shown in Fig. 4b. The third way was to combine the above two methods to conduct the two methods alternately—using a bar coater to coat 0.5 ml of solution firstly, and then after the surface was fully dried, conducting drop coating with a syringe to coat another 1 ml of solution. The reason for not using spin coating was to avoid much waste of the solution, and multiple times of conduction leading to much lower efficiency.

Figure 4c shows the samples' surface morphologies when using drop coating and bar coater coating. It is obvious that drop coating resulted in higher surface roughness than bar coater coating, as shown in Fig. 4d. This roughness is different from the roughness in Sect. 3.1 that indicates the dispersion of solutes, but has proved to be one

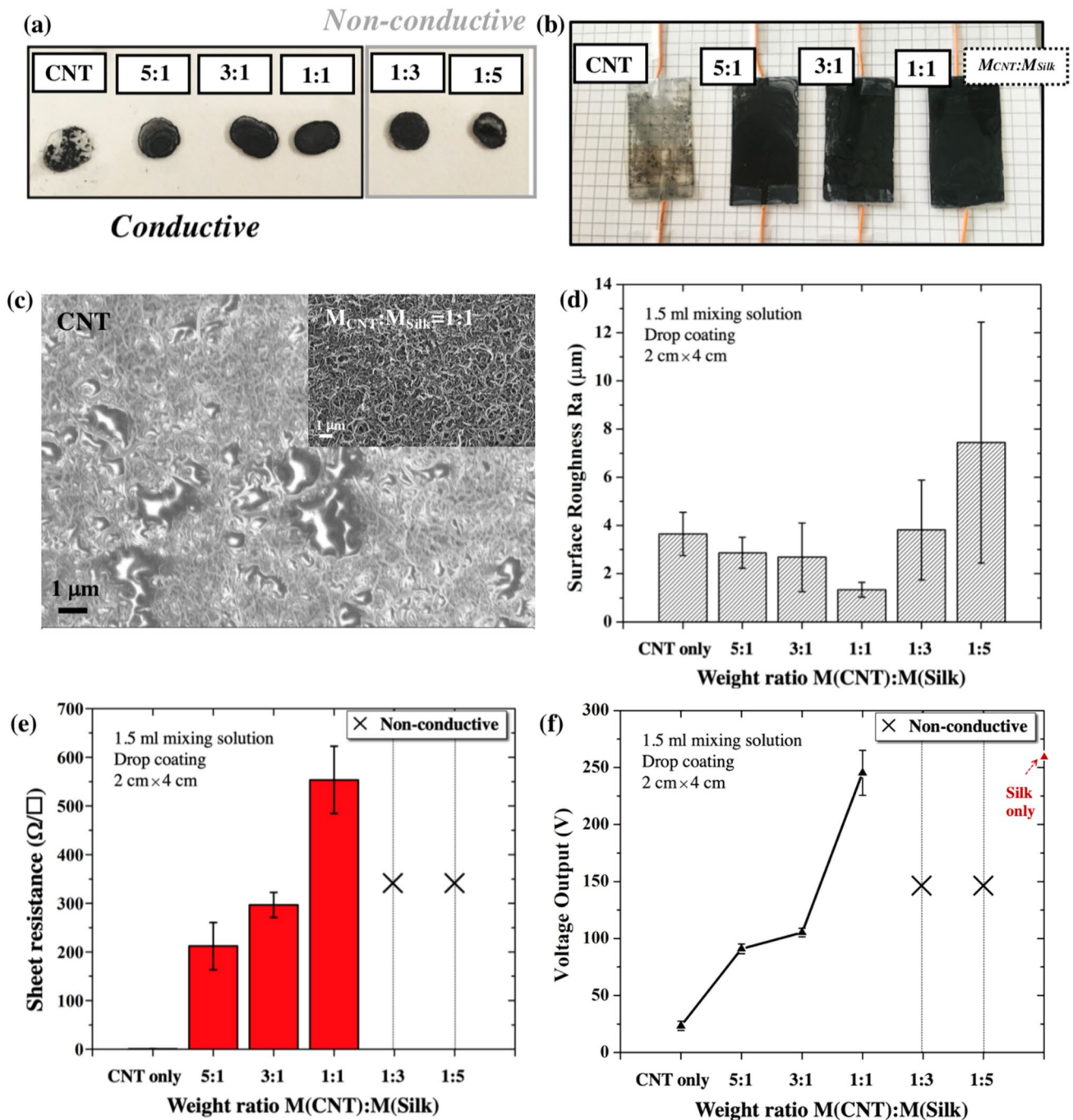


**Fig. 3** **a** The image of drop testing of the mixing solutions in different weight ratios. Each drop has the volume of 2  $\mu\text{l}$ . **b** Based on the conductive results from (a), the conductive solutions were coated on PET substrate, to fabricate the testing TENGs. **c** The surface morphology shows the agglomeration phenomenon of pure carbon nanotube layer. The right upper smaller view shows the surface morphology of mix-

ing solution in the ratio of 1:1. **d** The surface roughness, **e** the sheet resistance and **f** the output voltage of different TENGs fabricated with mixing solutions in different weight ratios, are the standards for comprehensive evaluation of the optimal ratio. It can be seen from the figures that 1:1 is the optimal choice for the best of three worlds

of the key parameters improving the output performance of TENGs, as shown in Fig. 4e. When this surface roughness increases, the effective friction area will be larger due to more surface patterns. On the other hand, the flat and

tight surface coated by the wire bar coater had much better durability according to the photos shown in Fig. 4e. Therefore, conducting the two methods alternately was chosen

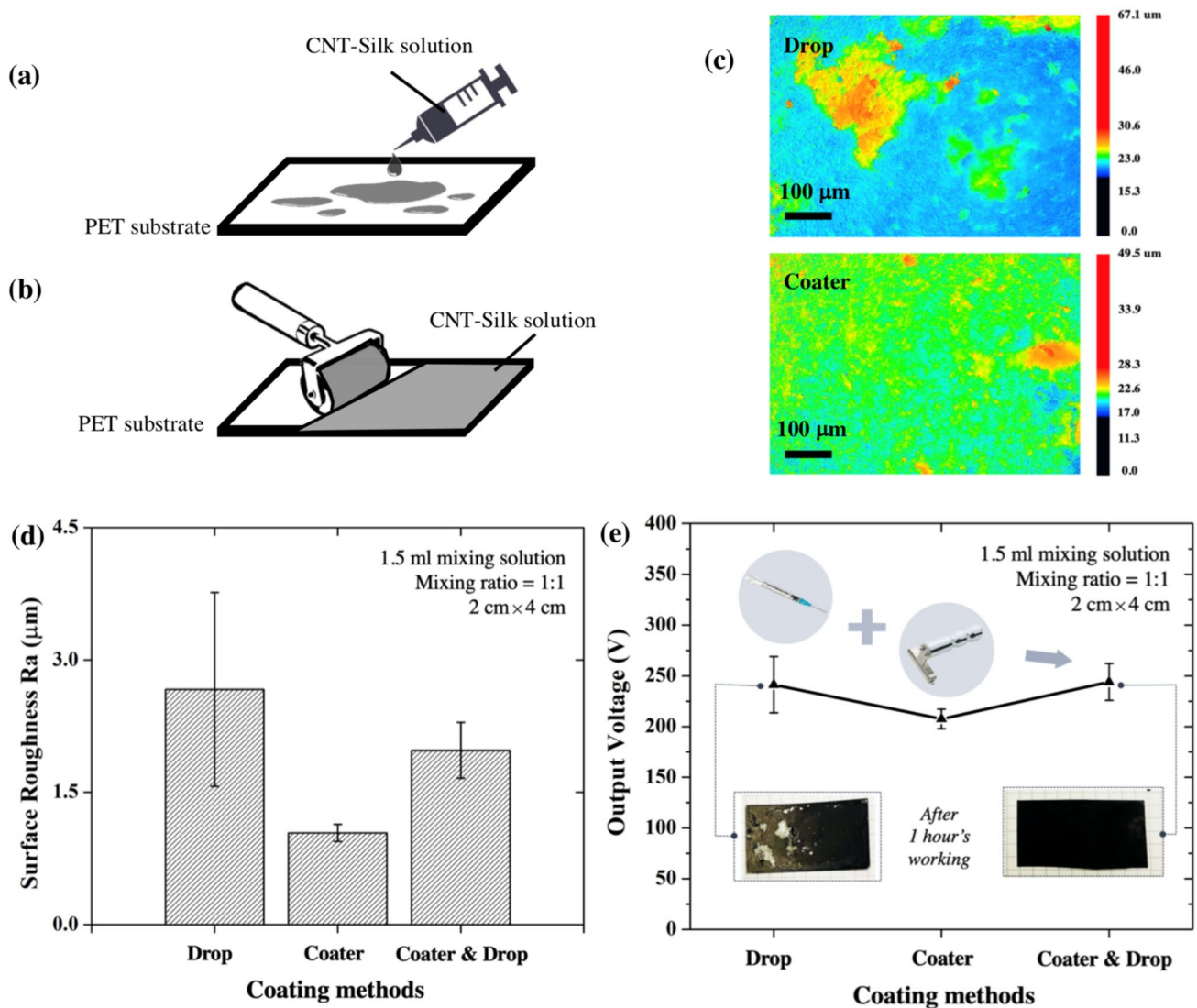


**Fig. 4** **a** The schematic view of drop coating with a syringe. **b** The schematic view of slide coating with a bar coater. **c** The surface morphology of the mixing layers coated by syringe drop coating and coater slide coating, respectively. **d** The surface roughness of the mixing layers coated by different coating methods. **e** The electric output

of the mixing layers coated by different coating methods. Although the power generation performance of the drop-coating layer and mix-coating layer was similar, the difference of durability could be seen from the sample's photos shown in **e**

as the proper choice, to achieve a stable bottom layer and a rough upper layer for better performance.

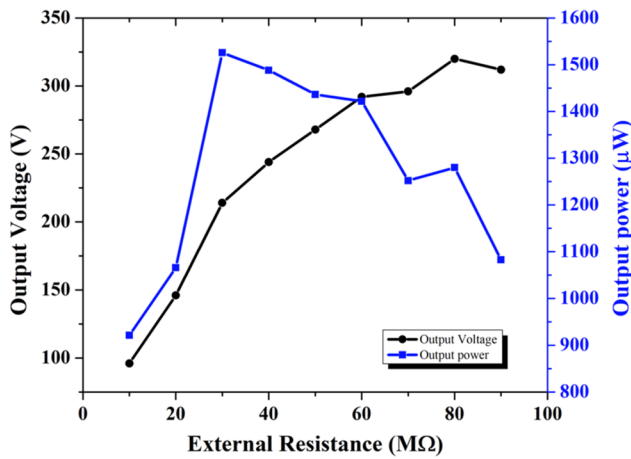
### 3.4 Electric Properties of PET-Substrate CNT-Silk TENG

According to the above experiments, the optimal values of certain parameters/conditions were obtained and verified. Therefore, the TENG used in the following tests were all based on the determined parameters/conditions to make sure of its best power generation performance. The electric properties of the fabricated CNT-silk testing TENG were

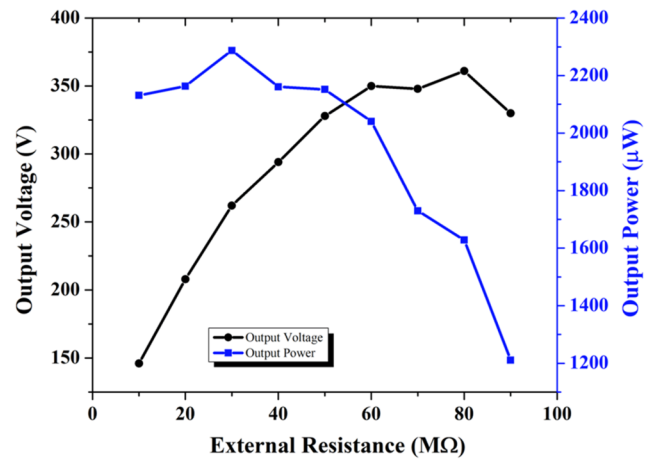
systematically investigated by using both a vibration platform and body motion (i.e. finger pressing).

The shaker introduced in Sect. 2.2 provided a stable external force of 14.7 N with a frequency of 7 Hz to the TENG. As shown in Fig. 5a, the output voltage of the connecting resistor increases continuously as its resistance increases from 10 to 90 MΩ, but the increase rate of the output voltage declines. Thus, the curve for the output power of the connecting resistor shows a single-peak profile in Fig. 5a, and the maximum value was achieved when the resistance value of the resistor was 30 MΩ with an electric output of 214 V, 7.13 μA, and 190.73 μW/cm<sup>2</sup>, respectively. The same samples were tested by hand

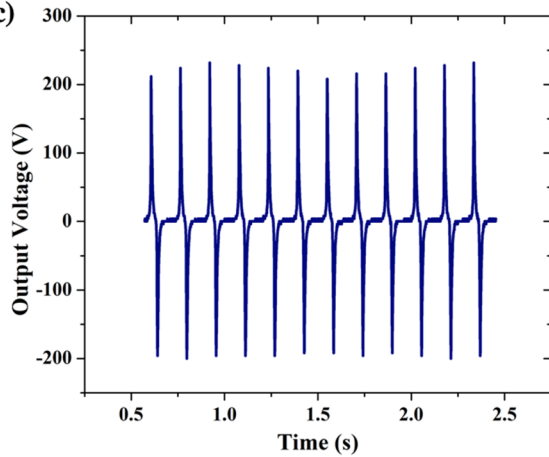
(a) **Shaker Patting**



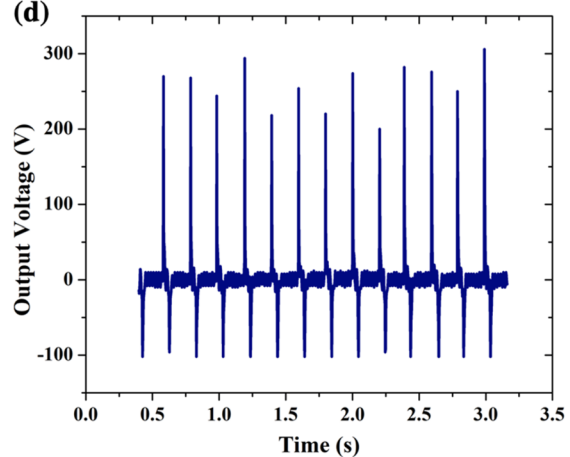
(b) **Hand Patting**



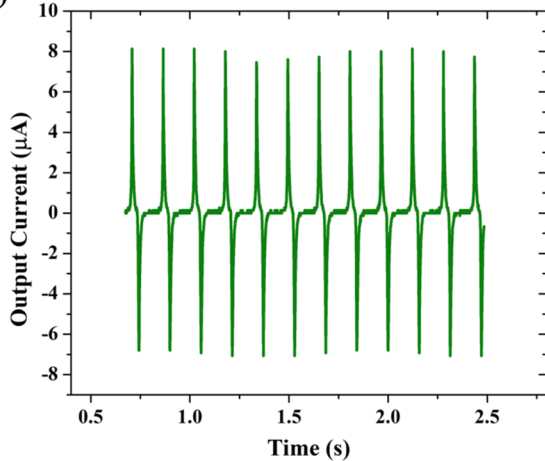
(c)



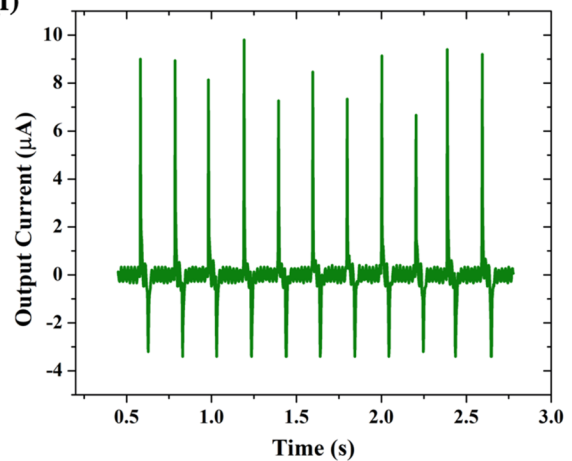
(d)



(e)



(f)



patting as well. The external force provided by hand patting was about 7 Hz, 20 N, a little stronger than that from shaker patting. As shown in Fig. 5d, f, the output reached 262 V and 8.73 μA, respectively, with a matched load of

30 MΩ. The power density reached a maximum value of 285.91 μW/cm<sup>2</sup>, which is sufficient to support many newly developed micro/nano electronic devices [46, 47].



**Fig. 5** The working ability of the CNT-silk testing TENG was systematically investigated by regularly patting from vibrational shaker and randomly patting from human hand. **a** The output voltage and output power corresponding to different external resistance under shaker patting. **b** The output voltage and output power corresponding to different external resistance under hand patting. Under shaker patting, **c** the output voltage and **e** current of fabricated testing TENG achieved averagely 214 V and 7.13  $\mu\text{A}$ , respectively, with a matched load of 30 M $\Omega$ . Thus, the output power achieved to the maximum value of 1.53 mW with the surface area of 8 cm<sup>2</sup>. Under hand patting, **d** the output voltage and **f** current of fabricated testing TENG achieved averagely 262 V and 8.73  $\mu\text{A}$ , respectively, with a matched load of 30 M $\Omega$ . Thus, the output power achieved to the maximum value of 2.29 mW with the surface area of 8 cm<sup>2</sup>

Then the TENG was used to directly charge a 7 nF capacitor without any external circuit for a charging ability testing. With one touch of 20 N which lasted for 0.03 s, an output voltage of 3.0 V was generated across the capacitor as shown in Fig. 6a, b, showing that the total amount of the charge generated by triboelectrification was approximately 21 nC, and an output current around 0.7  $\mu\text{A}$  was generated from one touch between the CNT-silk layer and the PET according to the formula

$$C = \frac{Q}{U} = \frac{\int I \cdot dt}{U}, \quad (1)$$

in which C is the capacity of the external capacitor, Q is the amount of charge generated by triboelectrification, U is the voltage across the external capacitor, and I is the average magnitude of the current generated by triboelectric charging during the time of t.

The fabricated testing TENG was furthermore tested by charging and fulfilling a 470 nF capacitor via a full-wave rectifier bridge to see its practical charging ability. The TENG fulfilled the capacitor within 1 min, as shown in Fig. 6c, d.

The fabricated TENG also successfully lighted up 57 LEDs connected in series, as is shown in Fig. 6e. A Christmas tree shape was displayed by the LED array when the TENG was driven by fingers.

The durability of the fabricated TENG was also tested for continuous operation by using the vibration platform for 180 min. After 75,600-cycle of beating with an external force, the output voltage of the TENG was almost unchanged with a slight decrease of 16.7%, as shown in Fig. 7a. The mixing layer after 180 min of operation was 2.3  $\mu\text{m}$  thinner than that before operation, as shown in Fig. 7c.

All of the above tests were performed at a default room temperature of 22 °C and a relative humidity of ~ 30%. Here, the power generation performance in higher humidity environments has also been tested. Figure 7b shows the results of a test using the system shown in Fig. 7d, which indicates that when the relative humidity exceeded 75%,

the power generation performance was greatly reduced. It is partly because that silk fibroin is soluble in water, so the consumption of friction material also affects the output. However, if the mixing film is subjected to alcohol annealing, the dissolution problem can be completely solved [48]. And when the humidity was too high, the charges generated by the friction were dispersed by the water vapor, resulting in very low power generation efficiency. But even in high humidity conditions, voltage outputs exceeding 100 V could be guaranteed. Suitable humidity for the human body in daily life is 30–60%, which is also a good range for this TENG's working.

Compared with the other wearable TENGs developed in recent years that similarly use the common materials in daily life, such as cotton (about 13  $\mu\text{W}/\text{cm}^2$ ) [29], parylene (39.37  $\mu\text{W}/\text{cm}^2$ ) [30] and pure silk (193.6  $\mu\text{W}/\text{cm}^2$ ) [40], the power generation performance of this device (285.91  $\mu\text{W}/\text{cm}^2$ ) is higher. Compared with other TENGs with higher output power, the materials used in this research are more suitable for daily consuming and wearing than PDMS (1.48 mW/cm<sup>2</sup>) [49], silicon rubber and nickel (0.89 mW/cm<sup>2</sup>) [36]. Although they are less vulnerable by using the strong materials, in terms of the purpose of wearing comfort and compatibility, the practicality is relatively weak. While having good power generation capability, the CNT-silk TENG also equips structural simplicity, economic universality and reproducibility, simultaneously.

### 3.5 Application

A large-area single-layer TENG was fabricated to demonstrate its high usability and potential application in daily life. As shown in Fig. 8a, a piece of CNT-silk film was attached to the glove, in order to avoid the impact of the human body on the test results at the demonstration stage. The layered structure is as shown in Fig. 8b. The CNT-silk layer and the external clothes/layer formed the proposed CNT-silk TENG. This was to test whether the proposed TENG could generate electricity from random friction between common materials shown in Fig. 8c, without the need of complicated mechanisms and motion modes. The whole process was conducted by hand-making without any extra processing or ultra-clean environment.

The first test was to use the mixing-layer-glove to gently tap a piece of polyester as shown in Fig. 9a, which is one of the most common fabrics in daily life. Because the force provided by a hand was as light as 0.5 N, the output tended to be random rather than stable. The highest voltage output was 67.2 V, as shown in Fig. 9c. Then, when the polyester was gently rubbed horizontally with the CNT-silk film, the output reached 36.4 V, as shown in Fig. 9d. In order to make the test more realistic, the tester grabbed the piece of polyester with the special glove to wipe something (e.g.

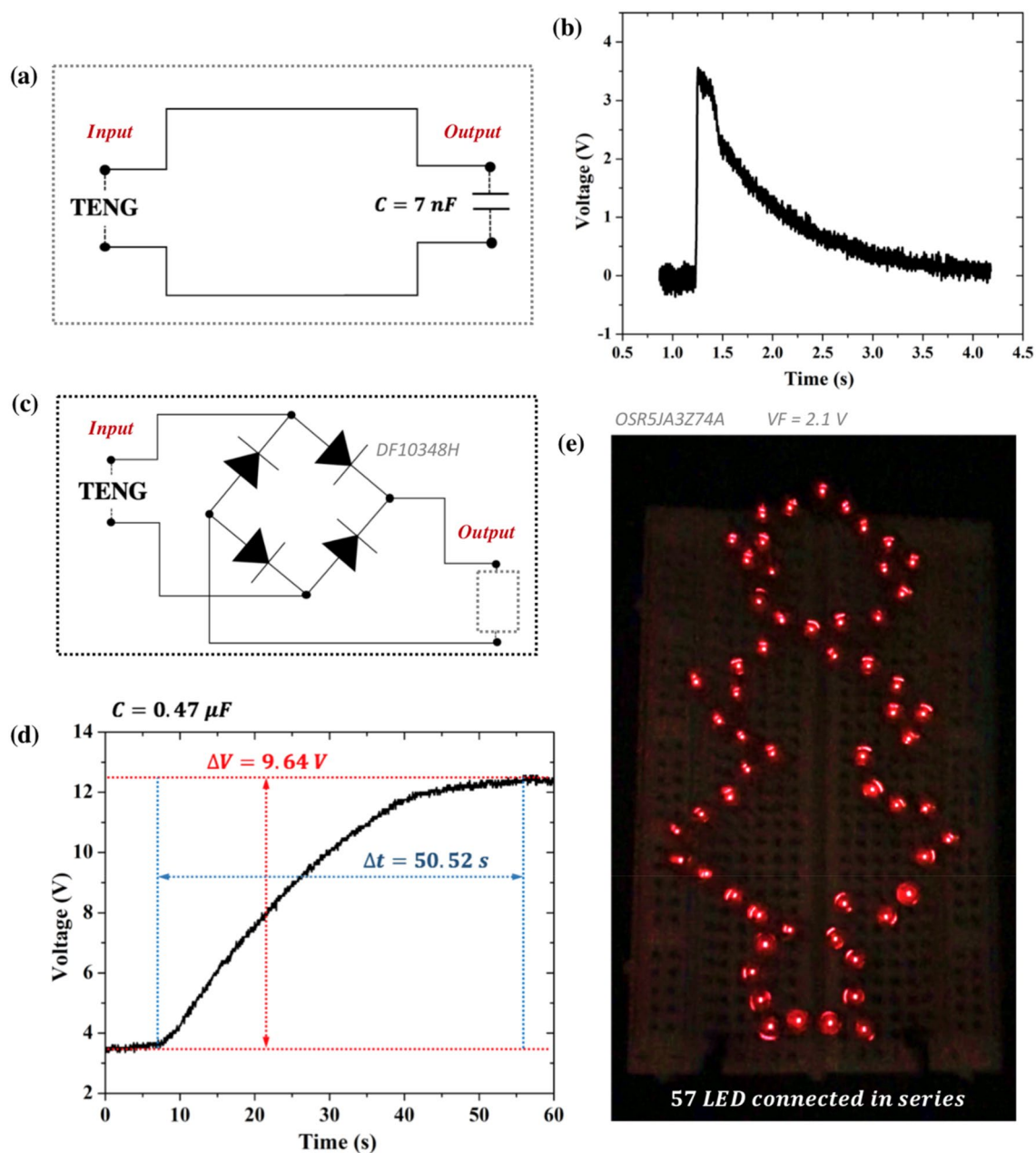


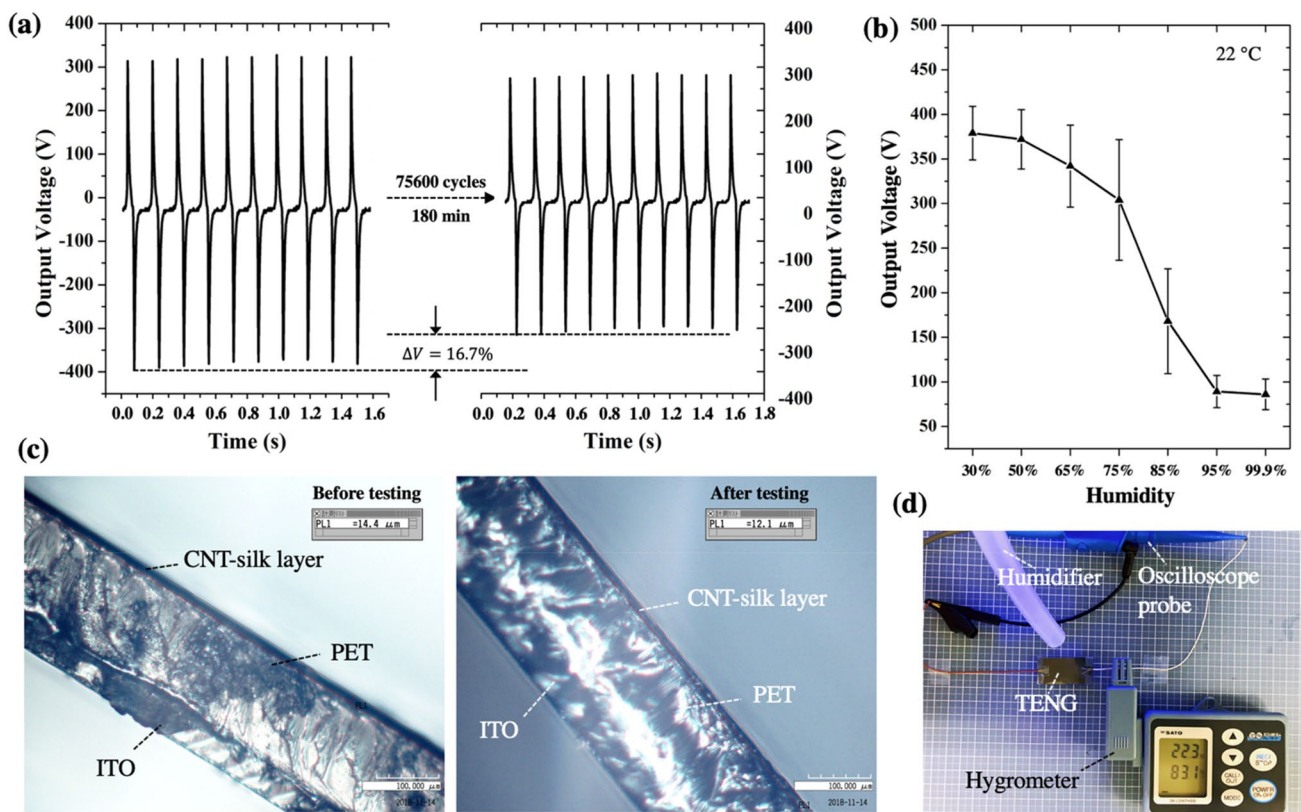
**Fig. 6** **a** The CNT-silk testing TENG was directly used to charge a 7 nF capacitor without any external circuit. **b** The waveform of the output voltage across the 7 nF capacitor generated by one touch between the mixing film and PET. **c** The amplifier circuit to convert

the AC signals delivered from the testing TENG into the DC signals. **d** The waveform of the amplified signals fully charging a 0.47  $\mu\text{F}$  capacitor within 1 min under hand patting. **e** The amplified signals of the testing TENG directly lighted up 57 LEDs under hand patting

screen of a mobile phone), as shown in Fig. 9e. Under these circumstances, there was almost no rubbing between the two friction materials, but the holding force was slightly changed with the swing of the fingers. Even in this case, the voltage output was obvious, reaching 14.4 V as shown in Fig. 9f.

Next, nylon was used as the second material to generate electricity. In the ranking of gaining and losing electrons, nylon is more likely to become positively charged than silk during friction. In this case, the mixing film was

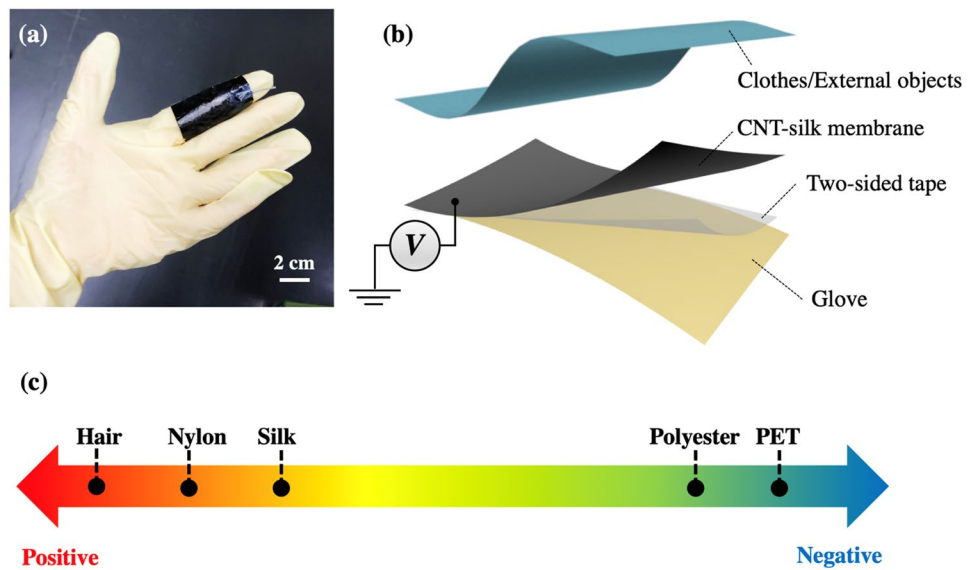
negatively charged. With very simple and casual pinching and rubbing with the force of about 1 N, the proposed TENG achieved an output voltage of 15 V, as shown in Fig. 10a, b. Last, the tester wore the special glove to gently flick her hair to further verify the wide applicability and high sensitivity to everyday actions, as shown in Fig. 10c. In a random touch on the hair, the proposed TENG reached a maximum voltage of 14.8 V as shown in Fig. 10d.



**Fig. 7** **a** The comparison of the output voltage of the testing TENG before and after 3 h working under shaker patting. The change of the thickness of the mixing layer before and after the 3 h working is shown in **c**. **b** The comparison of the output voltage under different

humidity with the room temperature of 22 °C. The setup was shown in **d**. The external vibration force in humidity tests was provided by hand patting

**Fig. 8** **a** A piece of CNT-silk mixing film of 2 cm × 4 cm was simply attached to the glove with two-side tape and connected to the measurement system by a wire. **b** A schematic view of the layered structure of the device shown in **a**. The CNT-silk layer and the external clothes/layer formed the proposed CNT-silk TENG. **c** The trend of losing or gaining electrons during friction of the materials in the following wearing tests



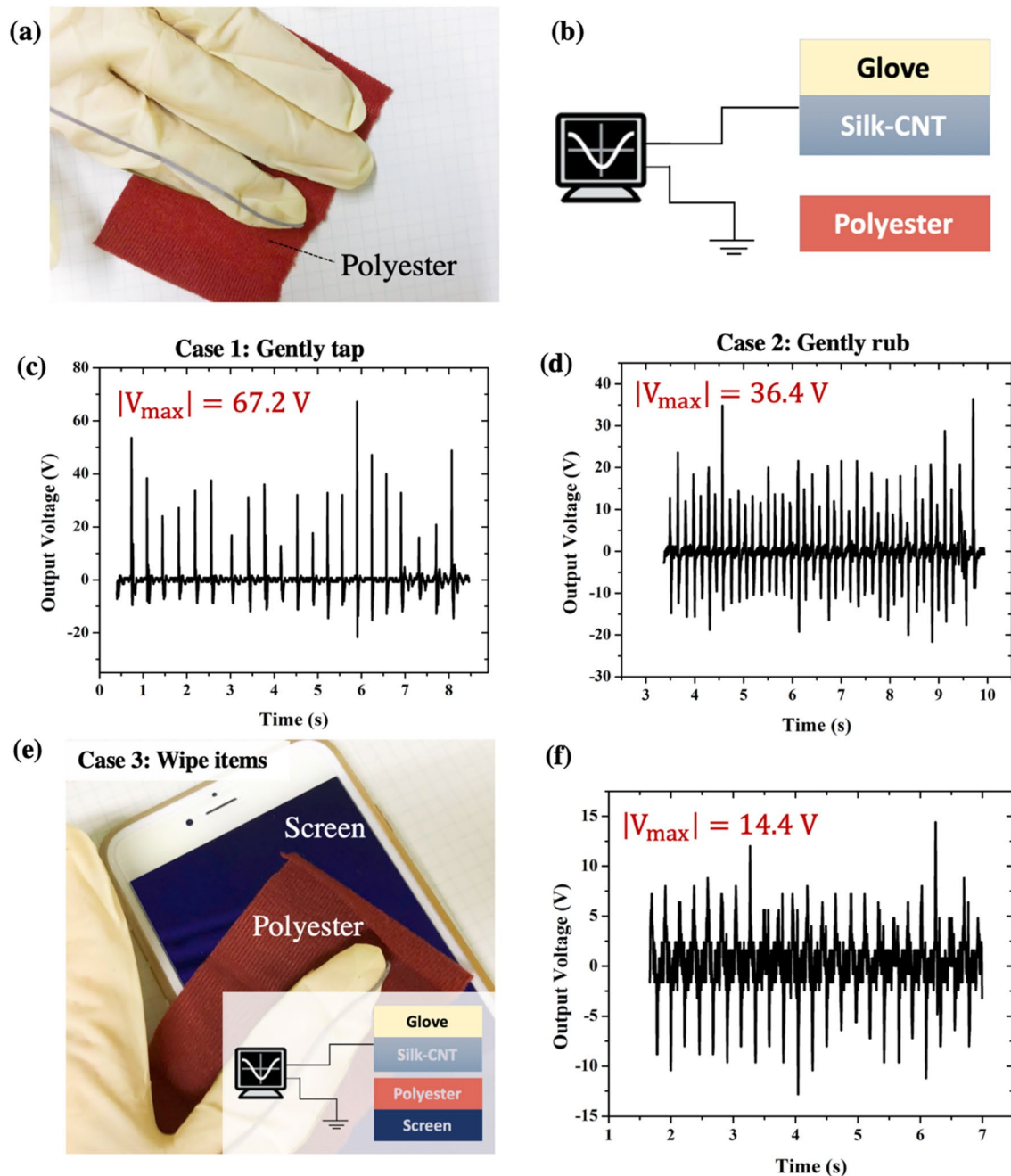


**Fig. 9** **a** Touching the polyester fabric by the glove with CNT-silk film. **b** The schematic view of the layer structure and circuit connection shown in **a**. **c** The output voltage during gently tapping by the glove on the polyester fabric. **d** The output voltage during gently rubbing by the glove on the polyester fabric. **e** Using the glove to hold a

polyester fabric to wipe a mobile phone screen, and the corresponding layer structure and circuit connection. **f** The output voltage during the action shown in **e**, with the two friction materials of CNT-silk mixing layer and polyester

Next, the same TENG system was used to charge a 7 nF capacitor, as shown in Fig. 11a. With one random touch less than 1 N, the voltage across the capacitor was tested. As shown in Fig. 11b–d, in the touch on polyester, nylon and human hair, the voltage of the capacitor reached 1.16 V, 1.92 V, and 0.36 V, respectively. Based

on Formula (1), it was calculated that during the moment of light contact, the amount of the generated charge were 8.12 nC, 13.44 nC, 2.52 nC, respectively. And accordingly, the generated current reached approximately 0.27  $\mu$ A, 0.45  $\mu$ A and 0.08  $\mu$ A, respectively. In daily life, such actions may be repeated many times in a short

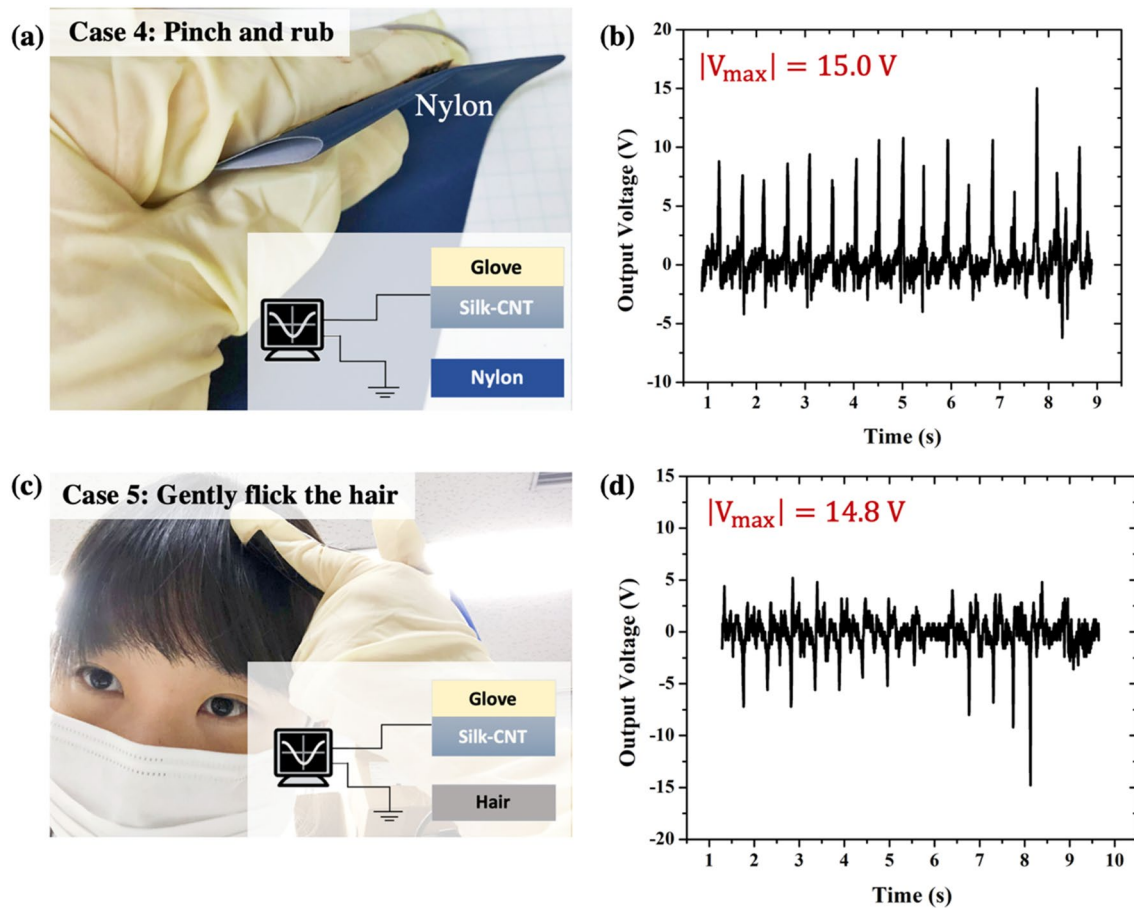


**Fig. 10** **a** Pinching and rubbing the nylon fabric by the glove with the mixing film, and the schematic view of the layer structure and circuit connection. **b** The output voltage during gently pinching and rubbing nylon by the glove with mixing film. **c** Gently flicking human hair by

the glove with the CNT-silk mixing film, and the schematic view of the layer structure and circuit connection shown in **c**. **d** The output voltage during gently flicking human hair by the glove with the mixing film

time, or may be performed simultaneously. If a capacitor was connected to the TENGs, when electricity was not needed, then charges could be accumulated through the motions in various local body places, and when electricity was needed, a higher current could be discharged in a short time to achieve more functions, such as powering sensors with higher power consumption, or microcurrent therapy [50].

According to the above experiments and demonstrations, it can be concluded that the CNT-silk film-based TENG has sufficient potential to act as a wearable device to provide power, or to be used as a motion sensor during various daily actions, with extremely high sensitivity, low cost, easy production, and high durability.

## 4 Conclusions

In summary, a novel, simply structured TENG with a hybrid mix of CNT and silk is first proposed. Two natural biodegradable materials, silk and CNT, were employed as the triboelectric material and electrode material, respectively. For the first time, the friction material and electrode material were combined in liquid phase, achieving a highly economical, accessible device which is great easy to be manufactured and integrated into clothes and wearable devices. A series of investigative experiments were conducted to clarify the impacts of various parameters and their optimal values in the fabrication, laying a solid foundation for further developments toward real applications and subsequent electrospinning experiments

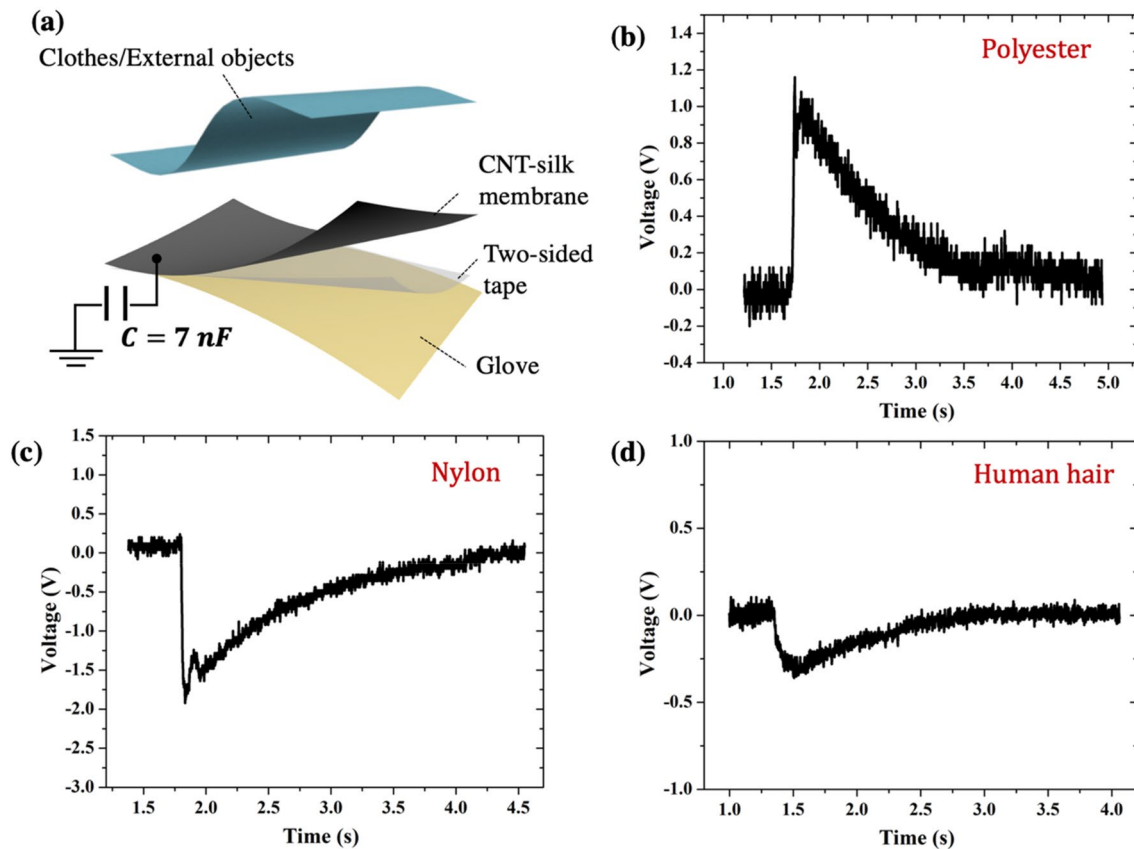


**Fig. 11** **a** Using the proposed CNT-silk TENG to charge a 7 nF capacitor, by contacting with polyester, nylon and human hair, respectively. The voltage of the 7 nF capacitor were tested when the glove touched **b** polyester, **c** nylon and **d** human hair once, respectively

to achieve textile/fibre structures with higher flexibility and stretchability.

The electrical features of the presented CNT-silk TENGs were comprehensively investigated by being fabricated into a PET-substrate testing mode, with a well-designed vibration platform and finger typing with a low frequency of 7 Hz. The fabricated TENG showed impressive stability under a 756,00-cycle continuous operation condition, with merely a 16.7% reduction in voltage. The voltage, current, and power density reached 262 V, 8.73  $\mu\text{A}$ , and 285.91  $\mu\text{W}/\text{cm}^2$ , respectively, with a matched load of 30 M $\Omega$ , which prove the CNT-silk film's capability in both biomechanical energy harvesting and self-powered active sensing.

Moreover, the proposed CNT-silk TENG was explored for generating power during daily actions. The experimental results proved that the CNT-silk film based TENG has sufficient potential to act as a wearable device to provide power, or to be used as a motion sensor during daily life, with extremely high sensitivity, low cost, easy production, and high durability. This new structure and its' fabrication method show attractive potential for simplifying the TENG structure and manufacturing process, thereby enhancing feasibility in further wearable

applications in smart clothes, healthcare sectors, portable electronics and many other fields.

**Acknowledgements** The authors thank Prof. Kimihiko Nakano and Nakano Laboratory members for their assistance with the vibration experiments, and the members of Kim Laboratory and Microsystems Laboratory 1 for helpful assistance and discussions.

**Author Contributions** The manuscript was written through contributions of all authors. All authors have given approval to the final version of the manuscript.

**Funding** This work was supported by the Global Leader Program for Social Design and Management (GSDM), the University of Tokyo; Japan Society for the Promotion of Science (JSPS) Core-to-Core A project 2019.

### Compliance with Ethical Standards

**Conflict of interest** The authors declare no competing financial interest.

## References

1. Yahya, F., Lukas, C., & Calhoun, B. (2018). A top-down approach to building battery-less self-powered systems for the internet-of-things. *Journal of Low Power Electronics and Applications*, 8(2), 21.
2. What exactly is the 'Internet of Things'?. <https://www.slideshare.net/Postscapes/what-exactly-is-the-internet-of-things-44450482>. Published Feb 9 2015, pp. 1–10.
3. Chen, H., Xue, M., Mei, Z., Oetomo, S. B., & Chen, W. (2016). A review of wearable sensor systems for monitoring body movements of neonates. *Sensors (Switzerland)*, 16(12), 1–17.
4. Zhu, Z., Liu, T., Li, G., Li, T., & Inoue, Y. (2015). Wearable sensor systems for infants. *Sensors (Switzerland)*, 15(2), 3721–3749.
5. Khalid, S., Raouf, I., Khan, A., Kim, N., & Kim, H. S. (2019). A review of human-powered energy harvesting for smart electronics: Recent progress and challenges. *International Journal of Precision Engineering and Manufacturing-Green Technology*, 6, 821–851.
6. Tian, W., Ling, Z., Yu, W., & Shi, J. (2018). A review of MEMS scale piezoelectric energy harvester. *Applied Science*, 8(4), 645.
7. Peng, S. W., Shih, P. J., & Dai, C. L. (2015). Manufacturing and characterization of a thermoelectric energy harvester using the CMOS-MEMS technology. *Micromachines*, 6(10), 1560–1568.
8. Yu, Y., Zhai, J., Xia, Y., & Dong, S. (2017). Single wearable sensing energy device based on photoelectric biofuel cells for simultaneous analysis of perspiration and illuminance. *Nanoscale*, 9(33), 11846–11850.
9. Bhosale, A., Anderson, A., & Deshmukh, P. S. (2018). Voltage enhancing using multi-magnetic arrangement for low frequency vibrational energy harvesting. *Journal of Vibroengineering*, 20(4), 1720–1732.
10. Lin, Z., Chen, J., & Yang, J. (2016). Recent progress in triboelectric nanogenerators as a renewable and sustainable power source. *Journal of Nanomaterials*, 2016, 5651613.
11. Kim, W., Bhatia, D., Jeong, S., & Choi, D. (2019). Mechanical energy conversion systems for triboelectric nanogenerators: Kinematic and vibrational designs. *Nano Energy*, 56, 307–321.
12. Hinchet, R., Seung, W., & Kim, S. W. (2015). Recent progress on flexible triboelectric nanogenerators for self-powered electronics. *Chemsuschem*, 8(14), 2327–2344.
13. Dalziel, C. F. (1972). Electric shock hazard. *IEEE Spectrum*, 9(2), 41–50. <https://doi.org/10.1109/mspec.1972.5218692>.
14. Kim, K., & Yun, K. (2019). Stretchable power-generating sensor array in textile structure using piezoelectric functional threads with hemispherical dome structures. *International Journal of Precision Engineering and Manufacturing-Green Technology*, 6, 699–710.
15. R. F. Yazicioglu, et al. (2009). Ultra-low-power wearable bio-potential sensor nodes. In *2009 annual international conference of the IEEE engineering in medicine and biology society*, pp. 3205–3208.
16. Haque, R. I., Farine, P. A., & Briand, D. (2018). Soft triboelectric generators by use of cost-effective elastomers and simple casting process. *Sensors and Actuators A: Physical*, 271, 88–95.
17. Xu, M., Wang, P., Wang, Y., et al. (2018). A soft and robust spring based triboelectric nanogenerator for harvesting arbitrary directional vibration energy and self-powered vibration sensing. *Advanced Energy Materials*, 8(9), 1–9.
18. Lee, D., Chung, J., Yong, H., et al. (2019). A deformable foam-layered triboelectric tactile sensor with adjustable dynamic range. *International Journal of Precision Engineering and Manufacturing-Green Technology*, 6, 43–51.
19. Bu, T., Xiao, T., Yang, Z., et al. (2018). Stretchable triboelectric-photonic smart skin for tactile and gesture sensing. *Advanced Materials*, 30(16), 1–8.
20. Chu, H., Jang, H., Lee, Y., Chae, Y., & Ahn, J. H. (2016). Conformal, graphene-based triboelectric nanogenerator for self-powered wearable electronics. *Nano Energy*, 27, 298–305.
21. Shahriar, M., Vo, C. P., & Ahn, K. K. (2019). Self-powered flexible PDMS channel assisted discrete liquid column motion based triboelectric nanogenerator (DLC-TENG) as a mechanical transducer. *International Journal of Precision Engineering and Manufacturing-Green Technology*, 6, 907–917.
22. Vo, C. P., Shahriar, M., Le, C. D., et al. (2019). Mechanically active transducing element based on solid-liquid triboelectric nanogenerator for self-powered sensing. *International Journal of Precision Engineering and Manufacturing-Green Technology*, 6, 741–749.
23. Park, J. J., Won, P., & Ko, S. H. (2019). A review on hierarchical origami and kirigami structure for engineering applications. *International Journal of Precision Engineering and Manufacturing-Green Technology*, 6, 147–161.
24. Lai, Y. C., Hsiao, Y. C., Wu, H. M., & Wang, Z. L. (2019). Waterproof-fabric-based multifunctional triboelectric nanogenerator for universally harvesting energy from raindrops, wind, and human motions and as self-powered sensors. *Advanced Science*, 1801883, 1801883.
25. Wang, X., Zhang, Y., Zhang, X., et al. (2018). A highly stretchable transparent self-powered triboelectric tactile sensor with metalized nanofibers for wearable electronics. *Advanced Materials*, 30(12), 1–8.
26. Oh, Y., Kwon, D., Eun, Y., et al. (2019). Flexible energy harvester with piezoelectric and thermoelectric hybrid mechanisms for sustainable harvesting. *International Journal of Precision Engineering and Manufacturing-Green Technology*, 6, 691–698.
27. Jang, S., Kim, Y., Lee, S., & Oh, J. H. (2019). Optimization of electrospinning parameters for electrospun nanofiber-based triboelectric nanogenerators. *International Journal of Precision Engineering and Manufacturing-Green Technology*, 6, 731–739.
28. Zhang, L., Yu, Y., Eyer, G., et al. (2016). All-textile triboelectric generator compatible with traditional textile process. *Advanced Materials Technologies*, 1(9), 1–8.
29. Pu, X., Li, L., Liu, M., et al. (2016). Wearable self-charging power textile based on flexible yarn supercapacitors and fabric nanogenerators. *Advanced Materials*, 28(1), 98–105.
30. Pu, X., Li, L., Song, H., et al. (2015). A self-charging power unit by integration of a textile triboelectric nanogenerator and a flexible lithium-ion battery for wearable electronics. *Advanced Materials*, 27(15), 2472–2478.
31. Dong, K., Wang, Y., Deng, J., et al. (2017). A highly stretchable and washable all-yarn-based self-charging knitting power textile composed of fiber triboelectric nanogenerators and supercapacitors. *ACS Nano*, 11(9), 9490–9499.
32. Choi, A. Y., Lee, C. J., Park, J., Kim, D., & Kim, Y. T. (2017). Corrugated textile based triboelectric generator for wearable energy harvesting. *Scientific Reports*, 7, 7–12.
33. Lai, Y. C., Deng, J., Zhang, S. L., Niu, S., Guo, H., & Wang, Z. L. (2017). Single-thread-based wearable and highly stretchable triboelectric nanogenerators and their applications in cloth-based self-powered human-interactive and biomedical sensing. *Advanced Functional Materials*, 27, 1.
34. Dong, K., Wang, Y., Deng, J., et al. (2017). 3D orthogonal woven triboelectric nanogenerator for effective biomechanical energy harvesting and as self-powered active motion sensors. *Advanced Materials*, 29(38), 1–11.
35. Seung, W., Gupta, M., Lee, K., et al. (2015). Nanopatterned textile-based wearable triboelectric nanogenerator. *ACS Nano*, 9(4), 3501–3509.

36. Tian, Z., He, J., Chen, X., et al. (2017). Performance-boosted triboelectric textile for harvesting human motion energy. *Nano Energy*, 39(May), 562–570.
37. Kim, K. N., Chun, J., Kim, J., et al. (2015). Highly stretchable 2D fabrics for wearable triboelectric nanogenerator under harsh environments. *ACS Nano*, 9(6), 6394–6400.
38. Song, J., et al. (2018). Highly flexible, large-area, and facile textile-based hybrid nanogenerator with cascaded piezoelectric and triboelectric units for mechanical energy harvesting. *Advanced Materials Technologies*, 3, 6.
39. Rasel, M. S., et al. (2018). An impedance tunable and highly efficient triboelectric nanogenerator for large-scale, ultra-sensitive pressure sensing applications. *Nano Energy*, 49, 603–613.
40. Zhang, X. S., Brugger, J., & Kim, B. J. (2016). A silk-fibroin-based transparent triboelectric generator suitable for autonomous sensor network. *Nano Energy*, 20(February), 37–47.
41. Rockwood, D. N., Preda, R. C., Yücel, T., Wang, X., Lovett, M. L., & Kaplan, D. L. (2011). Materials fabrication from *Bombyx mori* silk fibroin. *Nature Protocols*, 6(10), 1–43.
42. Kim, S., Marelli, B., Brenckle, M., et al. (2014). All-water-based electron-beam lithography using silk as a resist. *Nature Nanotechnology*, 9(4), 306–310.
43. Vepari, C., & Kaplan, D. L. (2009). Silk as a biomaterial. *NIH Public Access*, 32, 1–18.
44. Wang, S., Lin, L., & Wang, Z. L. (2012). Nanoscale triboelectric-effect-enabled energy conversion for sustainably powering portable electronics. *Nano Letters*, 12(12), 6339–6346.
45. Kim, J. H., Nam, K. W., Ma, S. B., & Kim, K. B. (2006). Fabrication and electrochemical properties of carbon nanotube film electrodes. *Carbon*, 44(10), 1963–1968.
46. MAX30208  $\pm$  0.1 °C Accurate, I2C Digital Temperature Sensor. <https://datasheets.maximintegrated.com/en/ds/MAX30208.pdf>.
47. Li, Z., Shen, J., Abdalla, I., et al. (2012). Ultra low power signal oriented approach for wireless health monitoring. *Sensors (Basel)*, 12(6), 7917–7937.
48. Minoura, N., Tsukada, M., & Nagura, M. (1990). Physico-chemical properties of silk fibroin membrane as a biomaterial. *Biomaterials*, 11(6), 430–434.
49. Marinkovic, S., & Popovici, E. (2017). Nanofibrous membrane constructed wearable triboelectric nanogenerator for high performance biomechanical energy harvesting. *Nano Energy*, 36, 341–348.
50. Cho, M. S., Park, R. J., et al. (2007). The effect of microcurrent-inducing shoes on fatigue and pain in middle-aged people with plantar fasciitis. *The Journal of Physical Therapy Science*, 19, 165–170.

(GSDM) since April 2016. She is currently engaged in the research of micro/nano energy technology.



**Jürgen Brugger** is Professor of Microengineering at the École Polytechnique Fédérale de Lausanne (EPFL), Switzerland. Before joining EPFL he was at the MESA+ Research Institute of Nanotechnology, University of Twente, The Netherlands, at IBM Zurich Research Laboratory, and at Hitachi Central Research Laboratory, in Tokyo, Japan. Since 1995, Dr. Brugger is active in the field of interdisciplinary and experimental micro and nanotechnologies with a focus on novel manufacturing

techniques for integrated and multi-functional micro/nanosystems. He served as co-chair of IEEE-MEMS 2015 and Program Chair of Transducers 2019. He is IEEE Fellow.



**Beomjoon Kim** is Professor of Institute of Industrial Science, the University of Tokyo, Japan. Also, he is currently a director of LIMMS/CNRS-IIS UMI 2820, at I.I.S., the University of Tokyo, since 2017. He received his B.E. degree from Seoul National University, Dept. of Mechanical Design and Production Eng., Korea, in 1993, and M.S., Ph.D. in Precision Engineering, from the University of Tokyo, Japan, in 1995 and 1998, respectively. He was a CNRS Associate Researcher in LPMO, Besancon,

France (1998–1999), and worked in MESA+ Research Institute, University of Twente (1999–2000). He was an Associate Professor in the Univ. of Tokyo (2000–2013), and was a co-director at the CIRMM/ CNRS Paris office (2001–2003).

**Publisher's Note** Springer Nature remains neutral with regard to jurisdictional claims in published maps and institutional affiliations.



**Meng Su** received her B.E. degree from Dalian University of Technology, School of Mechanical Engineering in July 2015, and her Master in Precision Engineering, from the University of Tokyo, Japan, in September 2017, respectively. She is currently a Ph.D. candidate in Precision Engineering, the University of Tokyo, Japan, since September 2017. She is a member of Global Leader Program for Social Design and Management